Finite Element Analysis with B-Splines: Weighted and Isogeometric Methods

Klaus Höllig, Jörg Hörner, and Axel Hoffacker

Universität Stuttgart, IMNG
Pfaffenwaldring 57, 70569 Stuttgart,
Germany

Abstract. Weighted and isogeometric methods use b-splines to construct bases for FEM. They combine the computational efficiency of regular grids with the geometric flexibility of CAD representations. We give a brief description of the key ideas of the two approaches, presenting them in a unified framework. In particular, we use b-spline nodes, to visualize the free parameters. Moreover, we explain how to combine features of both techniques by introducing weighted isogeometric finite elements. An error estimate for the resulting mixed method is given, and the performance of weighted approximations is illustrated by numerical examples.

Keywords: b-spline, finite element method, weight function, isogeometric approximation.

1 Introduction

B-splines play an important role in many areas of applied mathematics and engineering. With weighted[1] and isogeometric[2] methods, the advantages of the b-spline calculus are made available also to finite element techniques. Moreover, the new concepts provide a natural link from numerical simulation to geometric modeling where b-splines have long become a standard tool.

The two approaches are described in detail in the books *Finite Element Methods with B-Splines* [10] and *Isogeometric Analysis* [7], respectively. We also refer to [8,3,1,4] for a small sample of recent developments. In this paper, we give a brief introduction to some key ideas of both techniques, illustrating their basic features in the simplest possible setting. Moreover, we explain when a combination of both methods might be useful. We propose weighted isogeometric approximations which can, in particular, handle trim curves and surfaces efficiently. Of course, we would like to stimulate the interest of the reader to learn about all aspects of b-spline based finite elements, to implement algorithms for further applications, and to participate in the future development of the theory.

[1] Weighted extended b-splines (web-splines) were introduced by U. Reif, J. Wipper and the first author [12], cf. also http://www.web-spline.de

[2] Isogeometric Analysis was founded by T.J.R. Hughes, J.A. Cottrell, and Y. Bazilevs [14] .

J.-D. Boissonnat et al. (Eds.): Curves and Surfaces 2011, LNCS 6920, pp. 330–350, 2012.

We begin by reviewing basic facts about finite elements and b-splines (cf., e.g., [20,21,5,18]). In particular, we describe the concept of b-spline nodes, which is convenient for visualizing the degrees of freedom of numerical approximations. Then, weighted b-spline bases, isogeometric elements, and a new mixed method are discussed in turn. Moreover, we show that weighted isogeometric (mixed) elements approximate with optimal order. Finally, examples are presented which illustrate the performance of b-spline based simulations.

2 Finite Element Approximation

Many physical or engineering problems admit a variational formulation. This means that the function

$$x \mapsto u(x) \in \mathbb{R}$$

describing a phenomenon or process on a domain $D \subset \mathbb{R}^d$ minimizes an energy functional

$$u \mapsto \mathcal{Q}(u) = \int_D F(x, u, \nabla u, \ldots)\, dx$$

over a suitable Hilbert space H, which incorporates boundary conditions if necessary.

A finite element approximation

$$u_h = \sum_k c_k B_k$$

minimizes $\mathcal{Q}$ over a finite dimensional subspace $V_h = \operatorname{span}_k B_k$ of H:

$$\mathcal{Q}(u_h) = \min_{v_h \in V_h} \mathcal{Q}(v_h)\,,$$

where the discretization parameter h usually denotes a grid width. Clearly, the choice of V_h as well as of the basis functions or finite elements B_k is crucial for the accuracy and the efficiency of the resulting method. An enormous number of different possibilities is available – we will add several further choices in the next sections!

As a basic example, we consider Poisson's problem corresponding to

$$F = \frac{1}{2}\,|\nabla u|^2 - f(x)u\,,$$

with a given function f. If no boundary condition is imposed, the normal derivative of a solution u vanishes on the boundary ∂D. This so-called natural boundary condition does not have to be incorporated into the finite element subspace. A typical essential boundary condition is

$$u(x) = 0, \quad x \in \partial D\,. \tag{1}$$

It must be satisfied (at least approximately) by all elements of V_h, in particular by the basis functions B_k.

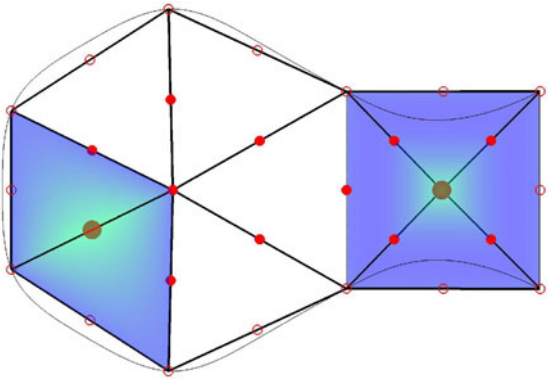

Fig. 1. Quadratic Lagrange elements on a triangulation

The standard classical finite element approximation of Poisson's problem on a two-dimensional domain D employs Lagrange elements on triangles. As is depicted in Figure 1, the degrees of freedom can be visualized by nodes at the positions of the interpolated values. To each node x^k corresponds a basis function B_k with $B_k(x^k) = 1$ and $B_k(x^\ell) = 0$ for $\ell \neq k$. The supports of two such finite elements are highlighted in the figure. The boundary condition (1) is imposed simply by assigning the value 0 to the boundary nodes (circles), leaving merely the values at the interior nodes (dots) as free parameters.

3 B-Splines

A (standard) d-variate b-spline b_k is a positive, bell-shaped, piecewise polynomial function of coordinate degree n. As is illustrated in Figure 2, smoothness and support are determined by the knots. The left figure visualizes the values of the b-spline by coloring the support on the grid. This style of graphic representation will be frequently used in the following. As shown on the right figure, cross sections of the graph coincide with scaled univariate b-splines.

It is convenient to associate a node x^k equal to the Greville abscissa with a b-spline b_k, i.e., x^k_ν is the average of the interior knots in the ν-th coordinate direction ($\nu = 1, \ldots, d$), counting multiplicities. The index $k = (k_1, ..., k_d)$ corresponds to the position of b_k on the grid separating the polynomial segments. Intuitively, the location of the node coincides with the point of strongest influence of the b-spline. The nodes will be used later on to visualize the degrees of freedom for spline approximations.

A spline is a linear combination of b-splines which have support on a grid-conforming hyper-rectangle R:

$$p = \sum_{k \sim R} c_k b_k \,,$$

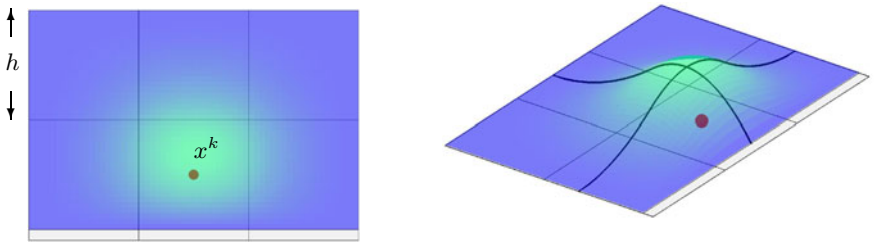

Fig. 2. Bi-quadratic b-spline with grid and node

where $k \sim R \Leftrightarrow k_\nu = 1, \ldots, m_\nu$ with $m_\nu + n + 1$ the number of knots in the ν-th coordinate direction. We can associate the free parameters or coefficients c_k with the b-spline nodes. Figure 3 shows two standard situations. Uniform splines (left) are spanned by translates of a single b-spline with obvious computational advantages. In particular, the node pattern is completely regular. For a boundary-conforming spline space (right), the boundary grid hyperplanes coincide with the boundary of the hyper-rectangle and have multiplicity $n+1$. This implies that the values of p along any of the hyper-rectangle boundaries are determined by the coefficients corresponding to the boundary nodes. For example, if all of these coefficients are 0, then p vanishes along the entire boundary of R.

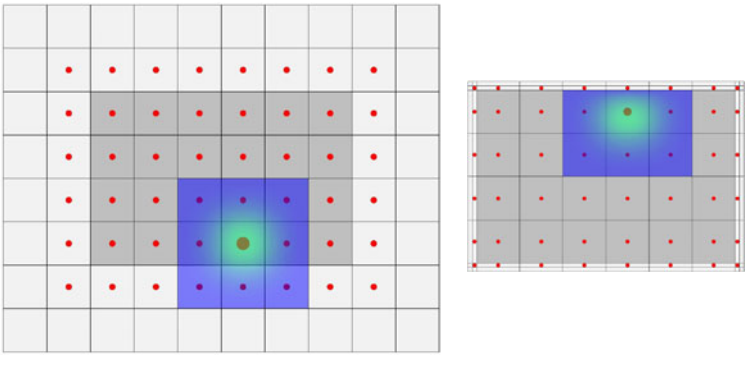

Fig. 3. Uniform and boundary-conforming bi-quadratic spline spaces

If the coefficients of a spline Φ are points $C_k \in \mathbb{R}^d$, then

$$\xi \mapsto x = \Phi(\xi) = \sum_{k \sim R} C_k b_k(\xi), \quad \xi \in R\,,$$

describes a transformation of the parameter hyper-rectangle R. The control net formed by the array of points C_k provides a qualitative description of the

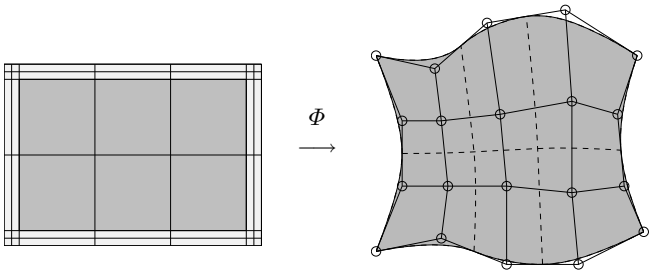

Fig. 4. Bi-quadratic b-spline parametrization with control net and grid

deformation caused by Φ, as does the isoparametric grid (image of the partition of the spline space under Φ).

Usually, boundary-conforming spline spaces are used for modeling parameter transformations as is the case for the example in Figure 4. The advantage is that the boundary of the image is determined entirely by the points C_k corresponding to the boundary nodes.

4 Weighted B-Splines

In order to approximate a function u on a domain D we can simply use splines defined on a hyper-rectangle R containing D:

$$u \approx u_h = \sum_{k \sim R} c_k b_k \,.$$

To emphasize that only those b-splines with some support in D are relevant, we set irrelevant coefficients to 0. In the example of Figure 5, uniform bi-quadratic b-splines are used; the solid relevant nodes correspond to the free parameters c_k, $k \sim D$.

Perhaps somewhat surprisingly, the simple procedure works well for unconstrained variational problems. Just restricting the b-splines to the simulation region D, provides very accurate finite element approximations u_h for problems with natural boundary conditions.

To incorporate essential boundary conditions, we resort to an idea already proposed by Kantorovich and Krylov [15]. We represent the domain D in implicit form via a weight function w,

$$D : w > 0 \,,$$

as illustrated on the left of Figure 5. Multiplying the b-splines b_k by w, we obtain a suitable finite element basis for constrained problems:

$$B_k = w b_k, \quad k \sim D \,. \tag{2}$$

By construction, any of the weighted elements satisfy $w(x)b_k(x) = 0$, $x \in \partial D$. The precise adaptation to the boundary is apparent from the sample elements highlighted on the right of the figure.

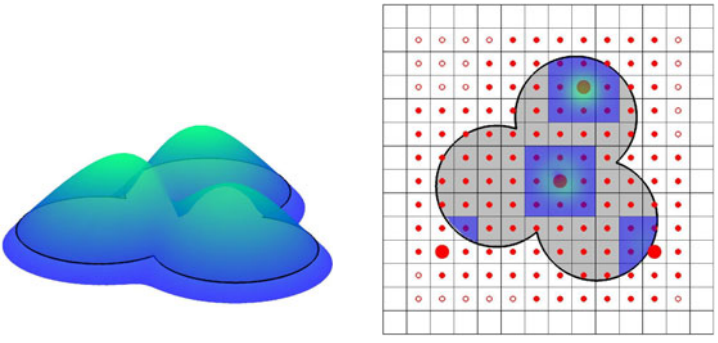

Fig. 5. Weight function and weighted bi-quadratic b-splines with grid and nodes

Weight functions can be constructed in various ways. For example, the smoothed distance to the boundary provides a general purpose solution. An elegant procedure is Rvachev's R-function method [17]. It combines elementary weight functions according to Boolean operations and is thus particularly well suited for simulations in conjunction with constructive solid geometry. The weight function on the left of Figure 5 was constructed in this fashion.

The weighted basis functions wb_k share all properties of standard finite elements, except for stability. For b-splines b_j, which do not have at least one of the grid cells of their support in D, the norm of wb_j is very small. For moderate grid widths this does not present any problems. In fact, the weighted basis (2) usually provides adequate approximations. However, for certain algorithms stability can be crucial, as $h \to 0$. To obtain stable finite elements, we combine neighboring b-splines with support near the boundary, forming so-called weighted extended b-splines (web-splines), introduced by U. Reif, J. Wipper, and the first author in [12]:

$$B_i = \sum_k e_{i,k}(wb_k), \quad i \in I\,.$$

The set I comprises all indices of inner b-splines, i.e., those b_i with at least one grid cell of their support in D.

The mathematics leading to the proper choice of the extension coefficients $e_{i,k}$ is somewhat subtle. However, the basis change $wb_k \to B_i$ can be implemented efficiently. In effect, the work amount is comparable to a sparse preconditioning procedure, since the (generalized) matrix $(e_{i,k})_{i\in I, k\sim D}$ has few off-diagonal entries.

In two variables, this construction is not even necessary. B. Mößner and U. Reif have made the surprising discovery that b-splines can be stabilized simply by scaling [16]. This is in agreement with many of our numerical experiments which indicated that stabilization can often be omitted. The scaling, proposed by B. Mößner and U. Reif, is inherent to most preconditioners for iterative solvers.

We reviewed in this section just the basic idea of the web-method, providing the prerequisites for the new mixed method, described in Section 6. A more

detailed introduction can be found on the web-site `www.web-spline.de` which also provides examples and further references.

5 Isogeometric Elements

Often it is possible to decompose a domain into simple patches which can be described as images of hyper-rectangles:

$$D = \bigcup_{\alpha} \Phi_\alpha(R_\alpha)\,.$$

In fact, CAD descriptions in solid geometry provide spline parametrizations of the form described in Section 3. A generalization of the classical isoparametric concept suggests itself. Isogeometric analysis, founded by T.J.R. Hughes, J.A. Cottrell, and Y. Bazilevs, provides a natural link from CAD models to FEM simulations. We briefly scetch the main idea of this powerful technique in a very simple setting, just providing sufficient detail to introduce a possible combination with weighted methods in the following section. For a comprehensive description of isogeometric analysis, we refer to [7].

As is illustrated in Figure 6, we can transform boundary-conforming b-splines defined on each of the hyper-rectangles R_α, with the aid of the mappings Φ_α. In other words, we use the basis functions

$$D \ni x \mapsto B_{k,\alpha}(x) = b_{k,\alpha}(\xi), \quad \xi = \Phi_\alpha^{-1}(x)\,,$$

the so-called isogeometric b-splines. Clearly, to ensure continuity, consistency at patch boundaries is crucial. This means that the restrictions of b-splines to a common patch boundary must coincide (nodes connected by red lines in the figure) and share the same coefficient.

We visualize the degrees of freedom by transforming the nodes associated with the b-splines to D,

$$\xi^{k,\alpha} \mapsto x^{k,\alpha} = \Phi_\alpha(\xi^{k,\alpha})\,,$$

as is illustrated in Figure 6. In particular, in view of consistency, nodes $x^{k,\alpha}$ on a common patch boundary are shared by the b-splines of the neighboring patches. Moreover, if essential boundary conditions are imposed as in the example in the figure, coefficients associated with nodes on outer boundaries (marked by circles) are set to 0.

It is convenient to also use boundary-conforming b-splines to represent the parametrizations Φ_α. Typically, the grid for the isogeometric elements then is a refinement of the grid for the parametrization. The degrees do not have to match. In the example in Figure 6, bi-quadratic b-splines are used throughout, which is, of course, a slight computational advantage. The basis functions $B_{k,\alpha}$ are slight perturbations of standard b-splines adapting to the grid determined by the mappings Φ_α.

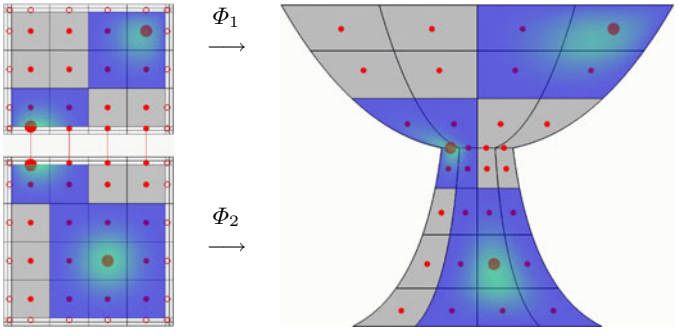

Fig. 6. Domain parametrization and bi-quadratic isogeometric b-splines with grid and nodes

Despite the nonlinear transformations involved, isogeometric methods can be implemented efficiently. Finite element integrals of the form

$$\int_D F(x, B(x), \nabla B(x), \ldots)\, dx, \quad B(x) = b(\xi),\ \xi = \Phi^{-1}(x)\,,$$

are computed over the relevant parameter hyper-rectangle R. By the chain rule and the formula for changing integration variables, the integral equals

$$\int_R F(\Phi(\xi), b(\xi), \nabla b(\xi)(J\Phi(\xi))^{-1}, \ldots)\ |\det J\Phi(\xi)|\ d\xi\,, \tag{3}$$

where $J\Phi$ denotes the Jacobi matrix of the transformation. Hence, matrix assembly does not require inverting the transformations of the parameter hyper-rectangles, a key feature familiar from classical isoparametric methods.

6 Weighted Isogeometric Approximation

Some commonly used CAD representations employ patches parametrized over trimmed parameter hyper-rectangles. A simple example is shown in Figure 7. To apply the standard isogeometric method, the image domain would have to be partitioned into deformed hyper-rectangles. As is already apparent from the elementary shape in the figure, it is not always easy to find a natural partition, in particular with few, only moderately distorted patches.

A possible remedy is a combination of the weighted and isogeometric approaches described, for the sake of simplicity, only for a single patch. We use weight functions to represent the trim curves or surfaces. The constraints can be specified either in the parameter hyper-rectangle R or the physical domain D. If both variants are used as in the example of Figure 7, the active portion R_a of the parameter domain consists of the points $\xi = \Phi^{-1}(x)$ with

$$w_R(\xi) > 0\,, \quad w_D(x) > 0$$

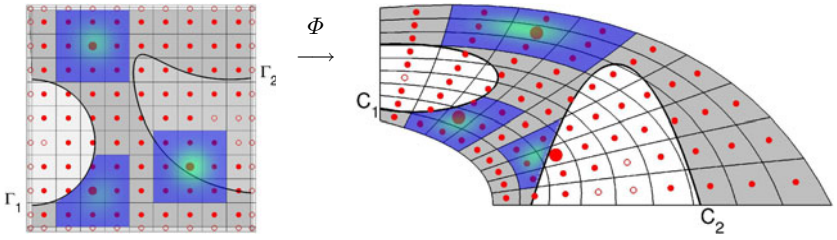

Fig. 7. Trimmed parameter rectangle and domain with bi-quadratic weighted isogeometric b-splines

($\Gamma_1 : w_R = 0$, $C_2 : w_D = 0$). Forming products with the boundary-conforming b-splines, we obtain the weighted isogeometric b-splines

$$x \mapsto B_k(x) = w_R(\xi) w_D(x) b_k(\xi), \quad x = \Phi(\xi)\,.$$

These basis functions are suited for problems with essential boundary conditions on the image of the trim curves or surfaces. If essential boundary conditions are also prescribed on the outer boundary of D, then the coefficients associated with the boundary nodes are set to 0. In Figure 7, the degrees of freedom are visualized in the usual way. The nodes $\xi^k \in R$ are transformed to the physical domain via $\Phi :\ x^k = \Phi(\xi^k)$.

Several weighted isogeometric b-splines B_k are highlighted on the right of Figure 7. As in the previous examples, degree 2 was used for the parametrization of the domain as well as for the b-spline basis. The weight functions coincide with the standard implicit representations of a circle and a parabola.

Trimming will usually lead to weighted isogeometric b-splines with small support within the domain D. To avoid the resulting instabilities, the stabilization measures, which were briefly mentioned at the end of Section 4, can be applied: simple scaling in two and extension in three variables [16,12]. This yields a stable basis if Φ and Φ^{-1} are smooth. It seems, however, that stabilization can be omitted in many cases. We have found (cf. the example at the end of the next section and the remark in connection with the first example in Section 8) that the accuracy of approximations is affected by instability only for extremely small grid widths.

Any weighted approximation requires special integration routines for boundary cells. This is straightforward in two dimensions (cf. [10], Section 8.4) for any degree and in three dimensions for degree 1, where an interesting preprocessing technique can be used (cf. [13]). Routines for three dimensional integration over cell intersections with general NURBS-domains have been developed (cf. the MIND project: `www.imng.uni-stuttgart.de/LstNumGeoMod/Hoerner/mind/`), and perform sufficiently well for smooth boundary portions. For complicated intersection patterns, as produced by curved edges and corners, integration can be time consuming. Fortunately, asymptotically (for small grid width), the percentage of these cases becomes small.

7 Error Estimate

We show in this section that weighted isogeometric approximations have, in general, the optimal approximation order for standard elliptic problems with smooth solutions. As a typical case, we consider Poisson's equation

$$-\Delta u = f$$

with mixed boundary conditions on a bounded domain $D \subset \mathbb{R}^d$ of the form shown in Figure 8 for $d = 2$. On the inner boundary C or trim surface, which encloses a simply connected subdomain, homogeneous Dirichlet boundary conditions are prescribed ($u_{|C} = 0$) and, on the outer boundary $\partial D \backslash C$, the solution satisfies the Neumann condition $\partial_\perp u = 0$ (vanishing normal derivative).

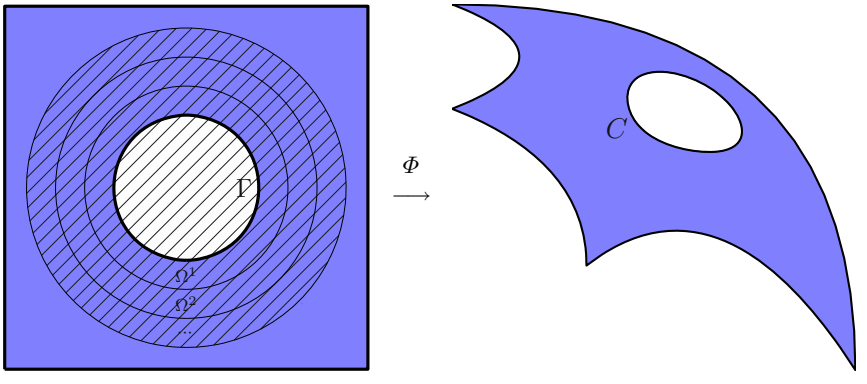

Fig. 8. Regularly parametrized domain $D = \Phi(\Omega)$, $\Omega \subset R$, with a smooth inner boundary $C = \Phi(\Gamma)$

We assume that the untrimmed domain is the image of a hyper-rectangle R under an $(n + 1)$ times continuously differentiable bijective transformation Φ with nonsingular Jacobian and denote by $\Omega = \Phi^{-1}(D)$ the trimmed parameter domain. Moreover, the trim surface C should be smooth, i.e., representable in implicit form via a smooth weight function w_D (or via $w_R = w_D \circ \Phi$ on the parameter hyper-rectangle R) with $w_D = 0 \wedge \operatorname{grad} w_D \neq 0$ on C and $w_D > 0$ in D and on the outer boundary. Under these hypotheses, the following error estimate holds.

Theorem (Error of Weighted Isogeometric Finite Elements). *The weighted isogeometric Ritz-Galerkin approximation u_h of degree $\leq n$ to a solution $u \in H^{n+1}(D)$ of the mixed Poisson problem described above satisfies*

$$\|u - u_h\|_{1,D} \leq \text{const}(D, w_D, \Phi, n)\, h^n\, \|u\|_{n+1,D}\,,$$

where $\|\ \|_{\ell,D}$ denotes the norm for the Sobolev space $H^\ell(D)$ of functions with square integrable ℓ-th order partial derivatives.

Proof. To simplify notation we use the symbols $\preceq, \succeq$ for inequalities with generic constants in one and both directions, which may depend on D, w_D, Φ, and n but neither on u nor on h. Moreover, we use a tilde for functions defined on the trimmed parameter hyper-rectangle $\Omega = \Phi^{-1}(D)$:

$$u(x) = \tilde{u}(\xi),\ u_h(x) = \tilde{u}_h(\xi),\ \ldots, \quad x = \Phi(\xi),\ \xi \in \Omega \subset R\,,$$

etc.

The proof relies on results and techniques from isogeometric analysis [2,7] and the theory of weighted approximations [12,10]; after all, the theorem pertains to a combination of key features of the two approaches. Moreover, the (by now!) standard error estimates for splines (c.f. the classical books by C. de Boor and L.L. Schumaker [5,18]) are crucial for our arguments. We refer also to [9], where a weaker version of the theorem was obtained, for some of the preliminary arguments.

We begin by noting that the composition with Φ or Φ^{-1} and multiplication by a smooth weight function w are bounded operations with respect to Sobolev norms:

$$\|p\|_{\ell,D} \preceq \|\tilde{p}\|_{\ell,\Omega} \preceq \|p\|_{\ell,D}, \quad \|wp\|_{\ell,D} \preceq \|p\|_{\ell,D}\,. \tag{S}$$

This elementary observation follows from the chain rule, the formula for transformation of multiple integrals, Leibniz' rule, and the fact that Φ, Φ^{-1}, and w are sufficiently smooth.

Now we observe that, by Cea's Lemma, the error of u_h can be bounded, up to a constant factor, by the error of the best approximation from the finite element subspace. Hence, it suffices to construct a linear combination

$$w_D v_h = \sum_k c_k\, w_D (b_k \circ \Phi^{-1})$$

of weighted isogeometric finite elements $B_k = w_D(b_k \circ \Phi^{-1})$, which approximates $u \in H^{n+1}(D)$ with the desired order:

$$\|u - u_h\|_{1,D} \preceq \|u - w_D v_h\|_{1,D}\,,$$

as just noted in the preceeding sentence.

By the first inequalities in (S), the change of variables induced by the parametrization Φ is bounded with respect to Sobolev norms. In particular,

$$\|u - w_D v_h\|_{1,D} \preceq_{(S)} \|\tilde{u} - w_R \tilde{v}_h\|_{1,\Omega}, \quad \|\tilde{u}\|_{n+1,\Omega} \preceq_{(S)} \|u\|_{n+1,D}\,.$$

Hence, we may construct the approximation on the parameter hyper-rectangle R.

An appropriate linear combination of weighted b-splines

$$w_R \tilde{v}_h = \sum_k c_k\, w_R b_k \approx \tilde{u}$$

($w_R\tilde{v}_h = (w_D v_h) \circ \Phi$, $w_R b_k = B_k \circ \Phi$) is simply obtained by choosing for $\tilde{v}_h = \sum_k c_k b_k$ a quasi-interpolant of

$$\tilde{v} = \tilde{u}/w_R\,.$$

Here, we use an extension of $\tilde{v}$ to all of $\mathbb{R}^d$ (also denoted by $\tilde{v}$) to avoid technical difficulties in the construction of quasi-interpolant functionals near the boundaries of Ω. The existence of bounded extensions with respect to Sobolev norms,

$$\|\tilde{v}\|_{\ell,\mathbb{R}^d} \preceq \|\tilde{v}\|_{\ell,\Omega}\,, \tag{E}$$

was established by Calderon and Stein [6,19].

Summarizing, after these preliminaries, to prove the theorem we have to show that

$$\|w_R\tilde{v} - w_R\tilde{v}_h\|_{1,\Omega} \preceq h^n \|\tilde{u}\|_{n+1,\Omega}, \quad w_R\tilde{v} = \tilde{u}\,. \tag{A}$$

It seems as if we are done (cf. also the remark after the proof) since multiplication by w_R is a bounded operation and the quasi-interpolant $\tilde{v}_h \approx \tilde{v}$ approximates smooth functions in the H^1-norm with order $O(h^n)$. This is indeed the case for pure one-patch isogeometric approximations (no weighting, $w_R \equiv 1$, $\tilde{v} = \tilde{u}$) in a very special setting. The main difficulty we are facing in the presence of essential boundary conditions on a trim surface is that $\tilde{u} \in H^{n+1}(\Omega)$ does not imply $\tilde{v} \in H^{n+1}(\Omega)$, i.e., $\tilde{v}$ is not sufficiently regular to yield the maximal quasi-interpolation order. The division by w_R in the definition of $\tilde{v}$ causes the loss of roughly one order of differentiation as is already apparent from univariate examples. This problem is overcome with techniques developed in [12] (cf. also [10], Section 5.5), in particular with two fundamental inequalities, which we restate for convenience of the reader in a form appropriate for the mixed boundary value problem under consideration.

For any subdomain $U \subset \Omega$ with distance $\delta > 0$ to the inner boundary $\Gamma = \Phi^{-1}(C)$, the functions $\tilde{v}$ and $\tilde{u} = w_R\tilde{v}$ satisfy

$$\|\tilde{v}\|_{n+1,U} \preceq \delta^{-1}\left(\|\tilde{u}\|_{n+1,U} + \|\tilde{v}\|_{n,U}\right)\,. \tag{R1}$$

Moreover,

$$\|\tilde{v}\|_{n,\Omega} \preceq \|\tilde{u}\|_{n+1,\Omega}\,. \tag{R2}$$

In the references cited, the estimates were given for a smooth weight function which vanishes to first order on the entire boundary (no Neumann part). They also apply in the present context since, in a neighborhood Ω' of the Neumann boundary ∂R, the weight function w_R is bounded from below by a positive constant. This implies that $\|\tilde{v}\|_{n+1,\Omega'} \preceq_{(S)} \|\tilde{u}\|_{n+1,\Omega'}$, i.e., near the Neumann boundary both estimates, which essentially pertain to boundary behavior, are trivial.

Proceeding with the estimate of the error of the quasi-interpolant $\tilde{v}_h \approx \tilde{v}$ (assertion (A)), we have to take the two different types of boundary conditions, Dirichlet and Neumann, into account; the inner and outer boundary have to be

treated in a slightly different fashion. To this end, we split the function $\tilde{v}$ to be approximated with the aid of a partition of unity into two parts:

$$\tilde{v} = \tilde{v}^D + \tilde{v}^N \,.$$

As is indicated by the superscripts, the support Ω^D of $\tilde{v}^D$ contains a neighborhood of the Dirichlet boundary Γ and the Neumann boundary ∂R is covered by $\operatorname{supp} \tilde{v}^N = \Omega^N$. More precisely, we choose $\Omega^D \subset R$ with positive distance from ∂R and $\Omega^N \subset (\Omega \cup {}^cR)$ with positive distance from Γ (cf. Figure 8). Moreover, the Sobolev norms of $\tilde{v}^D$ and $\tilde{v}^N$ are bounded in terms of the corresponding Sobolev norms of $\tilde{v}$. To accomplish this splitting, we choose two smooth nonnegtive functions (e.g., linear combinations of b-splines!) χ^D and χ^N with the appropriate supports and

$$\chi^D(\xi) + \chi^N(\xi) = 1, \quad \xi \in \mathbb{R}^d \,.$$

Then we set $\tilde{v}^D = \chi^D \tilde{v}$, $\tilde{v}^N = \chi^N \tilde{v}$. Clearly, by linearity, we have the same decomposition for the quasi-interpolants, i.e., $\tilde{v}_h = \tilde{v}_h^D + \tilde{v}_h^N$ ($\tilde{v}_h^*$ is a quasi-interpolant of $\chi^* \tilde{v}$).

As a final preparation for the main argument, we recall a standard estimate for quasi-interpolants $\tilde{p}_h$ with uniform b-splines b_k of functions $\tilde{p}$, defined on $\mathbb{R}^d$:

$$\|\tilde{p} - \tilde{p}_h\|_{m,U} \preceq h^{n+\nu-m} \|\tilde{p}\|_{n+\nu,U_h}, \quad 0 \le m \le n,\, \nu = 0, 1 \,, \tag{Q}$$

where U_h denotes the union of all b-spline supports overlapping the set U (actually, $\nu = m - n, \ldots, -1$ is possible; but not needed here). There exist many constructions for quasi-interpolants $\tilde{p}_h$; any of them which has the above approximation property is adequate for our purposes.

Referring to assertion (A), we now estimate each part (Neumann and Dirichlet) of the error

$$w_R \tilde{v} - w_R \tilde{v}_h = (w_R \tilde{v}^N - w_R \tilde{v}_h^N) + (w_R \tilde{v}^D - w_R \tilde{v}_h^D)$$

($w_R \tilde{v} = \tilde{u}$) in turn.

The estimate of the error for the Neumann part is straightforward:

$$\begin{aligned} \|w_R \tilde{v}^N - w_R \tilde{v}_h^N\|_{1,\Omega} &\preceq_{(S)} \|\tilde{v}^N - \tilde{v}_h^N\|_{1,\Omega_h^N} \preceq_{(Q)} h^n \|\tilde{v}^N\|_{n+1,\Omega^N} \\ &\preceq_{(E)} h^n \|\tilde{v}^N\|_{n+1,\Omega} \preceq_{(S)} h^n \|\tilde{u}\|_{n+1,\Omega} \,; \end{aligned} \tag{N}$$

the first inequality because $\operatorname{supp}(\tilde{v}^N - \tilde{v}_h^N) \subseteq \Omega_h^N$, the second inequality because $\operatorname{supp} \tilde{v}^N \subseteq \Omega^N$, the last inequality because $\tilde{v}^N = \chi^N \tilde{v} = \chi^N \tilde{u}/w_R$, χ^N is smooth, and $w_R \ge c > 0$ on $\Omega \cap \Omega^N = \Omega \cap \operatorname{supp} \chi^N$, noting that this set has a positive distance from Γ.

For analyzing the Dirichlet part in the decomposition of the error $w_R \tilde{v} - w_R \tilde{v}_h$, we introduce the abbreviation

$$w_R \tilde{v}^D - w_R \tilde{v}_h^D = w_R \tilde{e}_h \,,$$

i.e., $\tilde{e}_h$ is the error of the quasi-interpolant of $\tilde{v}^D$. To estimate the H^1-norm of $w_R\tilde{e}_h$, we have to take the weight function more explicitly into account. We use the inequality

$$\|w_R\tilde{e}_h\|_{1,U} \preceq \sup_{\xi\in U}|w_R(\xi)|\ \|\tilde{e}_h\|_{1,U} + \|\tilde{e}_h\|_{0,U} \tag{I}$$

which follows directly from the definition of the H^1- and L_2-norm and is valid for any subset U of Ω. Indeed, with $\|\ \|_0$ denoting the L_2-norm and by ∂_ν the partial derivative with respect to the ν-th variable,

$$\begin{aligned}\|we\|^2_{1,U} &= \|we\|^2_{0,U} + \sum_\nu \|\partial_\nu(we)\|^2_{0,U}\\ &\preceq_{(S)} \{\,\|e\|^2_{0,U} + \sum_\nu \sup_U|\partial_\nu w|^2\,\|e\|^2_{0,U}\,\} + \sum_\nu \sup_U|w|^2\,\|\partial_\nu e\|^2_{0,U}\,,\end{aligned}$$

where $\{\ldots\} \preceq_{(S)} \|e\|^2_{0,U}$ and the last term is $\le \sup_U|w|^2\,\|e\|^2_{1,U}$.

To capture the interplay between the smallness of w and the lack of regularity of $\tilde{v}$ near Γ, we cover $\Omega\cap\Omega^D_h$ (recall that Ω^D contains Γ and has a positive distance from the Neumann boundary ∂R) by strips Ω^1, Ω^2, ... with widths proportional to h and at least twice as large as the diameter of a b-spline support (cf. Figure 8). Using the inequality (I), we estimate $w_R\tilde{e}_h$ on each of these strips in turn. To this end the two terms on the right of the inequality are bounded with the aid of (Q), taking also the size of the supremum into account.

strip Ω^1: Since w_R is smooth and vanishes on Γ, we have $w_R(\xi) \preceq h$ on Ω^1. This implies

$$\begin{aligned}\|w_R\tilde{e}_h\|_{1,\Omega^1} &\preceq_{(I,Q)} h\,h^{n-1}\|\tilde{v}^D\|_{n,\Omega^1_h} + h^n\|\tilde{v}^D\|_{n,\Omega^1_h}\\ &\preceq_{(E,S)} h^n\|\tilde{v}\|_{n,\Omega} \preceq_{(R2)} h^n\|\tilde{u}\|_{n+1,\Omega}\,.\end{aligned} \tag{D1}$$

Here, (Q) was used with $m=1,\nu=0$ (first term) and $m=0,\nu=0$ (second term). We see that the inferior order for the H^1-norm of the error $\tilde{e}_h=\tilde{v}^D-\tilde{v}^D_h$ of the quasi-interpolant (first term) is compensated by the fact that w_R is small near the inner boundary Γ.

strips Ω^ℓ, $\ell>1$: By construction,

$$\delta = \operatorname{dist}(\Gamma,\Omega^\ell_h) \asymp \operatorname{dist}(\Gamma,\Omega^\ell) \asymp \ell h\,.$$

To this end we note that the width of Ω^1 is at least twice as large as a b-spline support, so that this assertion is valid in particular for Ω^2_h; the enlarged set does not touch Γ. Moreover, by our assumptions on the weight function, $w_R \preceq \ell h$ on Ω^ℓ_h. Hence, since $\delta^{-1} \preceq (\ell h)^{-1}$,

$$\begin{aligned}\|w_R\tilde{e}_h\|_{1,\Omega^\ell} &\preceq_{(I,Q)} (\ell h)\,h^n\|\tilde{v}^D\|_{n+1,\Omega^\ell_h} + h^{n+1}\|\tilde{v}^D\|_{n+1,\Omega^\ell_h}\\ &\preceq_{(S)} \ell h^{n+1}\|\tilde{v}\|_{n+1,\Omega^\ell_h} \preceq_{(R1)} h^n\left(\|\tilde{u}\|_{n+1,\Omega^\ell_h} + \|\tilde{v}\|_{n,\Omega^\ell_h}\right).\end{aligned}$$

Here, (Q) was used with $m = 1, \nu = 1$ (first term) and $m = 0, \nu = 1$ (second term). The fact that, for $\ell > 1$, Ω^ℓ and Ω_h^ℓ have a positive distance from Γ is crucial. This is the reason why the case $\ell = 1$ has to be treated differently.

Squaring the inequality, noting that $(\alpha + \beta)^2 \preceq \alpha^2 + \beta^2$, and summing over $\ell > 1$, we obtain the error bound also on the remaining part of the support Ω_h^D of $\tilde{e}_h$ within Ω:

$$\|w_R \tilde{e}_h\|^2_{1,\cup_{\ell>1}\Omega^\ell} \preceq h^{2n} \left(\|\tilde{u}\|^2_{n+1,\Omega} + \|\tilde{v}\|^2_{n,\Omega}\right) \preceq_{(R2)} h^{2n} \|\tilde{u}\|^2_{n+1,\Omega}\,, \qquad \text{(D2)}$$

noting that $\Omega_h^\ell \subset \Omega$ for small enough h and these enlarged strips overlap at most twice; $\Omega_h^\ell \cap \Omega_h^{\ell'} = \emptyset$ for $|\ell - \ell'| > 1$. Since

$$\Omega \cap \operatorname{supp} \tilde{e}_h = \Omega \cap \Omega_h^D \subset \cup_{\ell \geq 1} \Omega^\ell\,,$$

combining the estimates (D1,D2) yields the desired bound also for the Dirichlet part of the error. Together with the estimate (N) this proves (A) and thereby the theorem. □

The arguments have been somewhat technical. This reflects the complexity of the approximation process which involves b-splines of arbitrary degree, curved boundaries, parametrizations, and weight functions. However, we note that a substantially simpler argumentation is possible if one is content with an error estimate of the form

$$\|u - u_h\|_{1,D} = O(h^n)\,,$$

which does not show the precise dependence on the regularity of u. A result of this type neither requires the splitting of the error nor the regularity results (E), (R1), and (R2). With the aid of (Q) a relatively short proof is possible if one assumes, e.g., that u has continuous partial derivatives up to order $n + 2$. While we think that the above estimate is adequate for many purposes, usually, in finite element analysis, bounds with optimal regularity are preferred. They are essential for certain applications, e.g., the convergence analysis for multigrid algorithms, and certainly more appealing from an aesthetic point of view.

It is clear, that we can obtain analogous estimates for any standard elliptic second order problem with smooth solutions and smooth Dirichlet boundaries. More delicate (not done also for pure weighted approximations) is the analysis for problems with singularities due to reentrant corners or discontinuities and incompatible boundary conditions. As is well known, solutions are generally not smooth in these cases, unless the data satisfy appropriate conditions. Also not covered are singular parametrizations as well as non-smooth weight functions. The latter arise when applying Rvachev's technique for domains with corners (at least if the simplest R-function system is used). In this case one is confronted with lack of regularity of solutions as well and should note that using high degree b-splines (isogeometric or weighted) will not pay off for non-smooth problems (corners, discontinuities, singularities, etc.) unless suitable enhancements are used (e.g., additional special basis functions or adaptive refinement).

We have considered a single parametrization Φ since this is the case which is most relevant for the weighted isogeometric method. With our handling of trim

surfaces one can often avoid partitioning the domain. When several parametrizations are used (cf. Figure 6), the quasi-interpolation error has to be estimated separately for each deformed hyper-rectangle. Since, in general, parametrizations will merely join continuously, composition with Φ or Φ^{-1} is no longer globally bounded with respect to Sobolev norms. Hence, the arguments become much more elaborate, already without a weight function (see [2] for a comprehensive error analysis as well as a number of open questions mentioned in the introduction).

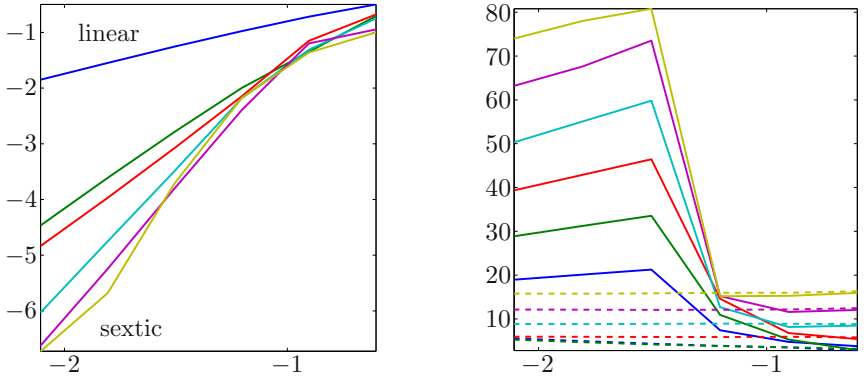

Fig. 9. Logarithmic plots of H^1-errors (left) and condition numbers (right) of weighted isogeometric Ritz-Galerkin approximations for the mixed Poisson problem with $f = 1$

We confirm the asserted convergence rates experimentally. The left diagram of Figure 9 shows the expected increase in accuracy with the degree. The logarithmic errors $\log \|u - u_h\|_{1,D}$ are plotted as functions of $\log h$; the labels show the decimal exponents. From the slopes we obtain estimates for the average rate, e.g., the rate approaches 5 for quintic approximations (degree 5). The computations were performed without extension, i.e., with the simple weighted isogeometric basis. We note that the instability has virtually no effect on the accuracy, despite huge condition numbers, as shown in the right diagram (solid lines). For example, the condition, estimated with the MATLAB `condest` command, exceeds 10^{70} for degree 6. This limited relevance of stability has been noticed in other examples. The phenomenon is probably due to the fact that preconditioning is inherent in many iterative solvers like the pcg-ssor routine used for this example. A theoretical explanation is given by B. Mößner and U. Reif [16], who showed that bivariate b-splines can be stabilized simply by scaling. Hence, at least in two variables, the extension procedure described at the end of Section 4 is, also from a theoretical point of view, not necessary.

The right diagram also shows the condition numbers for stabilized weighted extended isogeometric bases for degrees 1 to 6 (dashed lines at the bottom of the diagram). As expected the values are drastically smaller, reflecting the predicted order $O(h^{-2})$ for the condition of the Ritz-Galerkin system. In all cases, the condition numbers for the extended bases are $\leq 10^{20}$. Perhaps somewhat

surprisingly, not only the errors but also the number of pcg-ssor iterations are roughly identical for the stable and unstable case in this example; another indication of inherent preconditioning.

8 Applications

The true measure for comparing finite element software are complicated three-dimensional problems. We give examples for the weighted and weighted isogeometric b-spline techniques. For the pure isogeometric method we refer to the literature (cf., e.g., [7] and the references cited therein) since we have at this point only the simple one-patch discretization implemented which cannot handle complex geometrical structures.

Figure 10 shows a domain D with many holes, which is defined implicitly by a randomly generated piecewise trilinear weight function

$$D: \; w_h = \sum_k w_k b_k > 0 \, .$$

Clearly, only the weighted method will handle the complicated boundary pattern efficiently. As a test case, we solve the Poisson problem with essential homogeneous boundary conditions and

$$\mathcal{Q}(u) = \frac{1}{2} \int_D |\mathrm{grad} u|^2 - 2u \, .$$

Due to the irregular boundary, the regularity of the solution is poor. Hence, linear b-splines provide an adequate approximation:

$$u_h = w_h p_h, \quad p_h = \sum_k u_k b_k \, .$$

Using the same representation for the weight function w_h as well as for the spline p_h, leads to an appealing data structure. On each grid cell (cube with edge length h), the approximation u_h is determined by 2×2^3 values at the corners which coincide with the b-spline coefficients in this case. As a consequence, as is described in [13], a very efficient solution procedure is possible. For example, on a grid of $577^3 = 192,100,033$ unknowns, a dynamic vectorized multigrid solver on a NEC SX8 with 8 CPUs on one node reaches a relative residual less than $1E-8$ in < 50 seconds of real time. Perhaps even more striking is that the time for assembling the discrete finite element system (usually the bottle neck in simulations) is comparable to the time required by the solver. This demonstrates the excellent performance of assembly algorithms for b-spline based methods.

It is interesting to note that the multigrid iteration has been programmed without stabilization via extension. While stability of the basis is (to date!) essential for the convergence theory, our solver does not seem to require it; a simple diagonal preconditioning suffices, at least for this particular application (cf. also the remarks at the end of Section 7 and [16]).

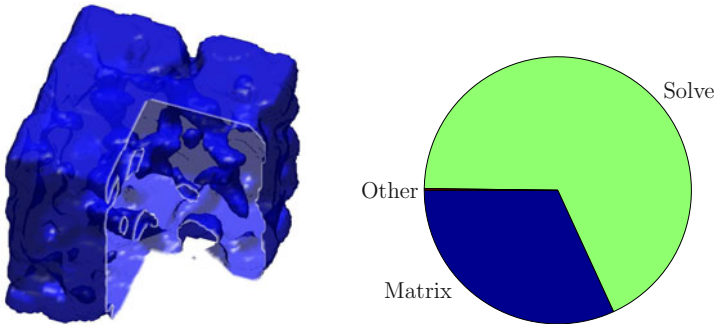

Fig. 10. Randomly generated domain for Poisson's problem and relative computing time of program components

In our second example, we consider the deformation of an elastic solid occupying a volume $D \subset \mathbb{R}^3$ under gravity. The displacement

$$(u_1(x), u_2(x), u_3(x)), \quad x \in D\,,$$

satisfies the Navier-Lamé system and minimizes the energy functional

$$\mathcal{Q}(u) = \frac{1}{2}\int_D \sigma(u) : \varepsilon(u) - fu\,,$$

where σ is the stress and ε the strain tensor.

We choose a geometric form which is neither ideally suited for weighted nor for isogeometric b-spline approximations. The curved bridge shown in Figure 12 has a relatively simple shape. Nevertheless both, the weighted and the isogeometric method, do not provide good discretizations as is illustrated in Figure 11. A straightforward description of the domain with a global weight function leads to unnecessary many boundary cells. On the other hand, while the principal shape is an absolutely elementary example of a deformed cuboid (a Bézier parametrization of coordinate degree $(1, 1, 2)$ suffices), the trim surfaces prevent the representation with a simple parametrization. Instead, a partition into deformed cubes is required (cf. [7], Figure 2.29 for a similar example), which does not reflect the simplicity of the geometry. As a consequence, one loses some of the computational efficiency; a vectorizable assembly routine is no longer applicable in a straightforward fashion.

The mixed method described in Section 6 suggests itself. We use a single polynomial parametrization Φ in Bézier form on a rectangle R and model the trim surfaces by a product of three elementary weight functions. In other words, we use finite elements of the form

$$e_\nu \left(\prod_{\alpha=1}^{3} w_\alpha(\xi)\right) b_k(\xi), \quad \nu = 1, 2, 3,\ k \sim R\,,$$

where the multiplication by the unit vectors e_ν takes the vector-valued form of the approximation u_h into account. As a consequence, we obtain fairly accurate

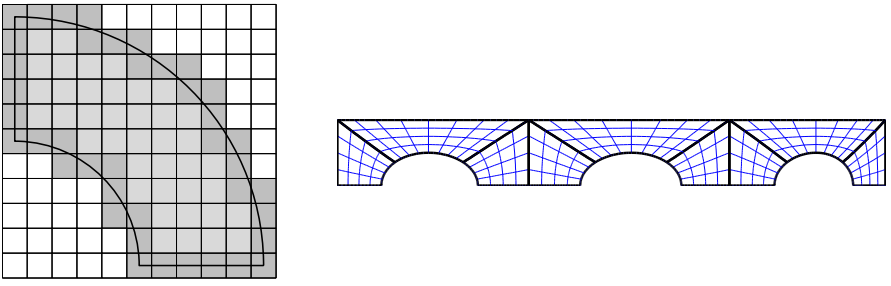

Fig. 11. Weighted (left, top view) and isogeometric (right, side view) discretization of a curved bridge

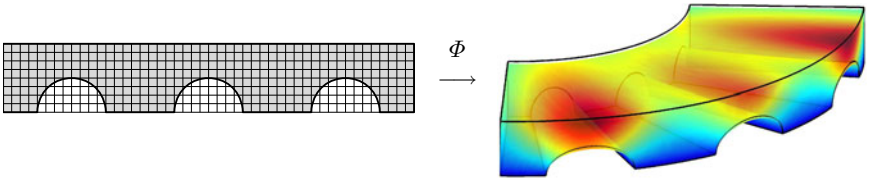

Fig. 12. Deformation of an elastic solid

numerical results with relatively few parameters. Figure 12 visualizes the magnified deformation for concrete (Young's modulus: $E = 50\,\mathrm{kN/mm^2}$, Poisson's ratio: 0.2). It was computed with $3 \cdot 50 \cdot 5 \cdot 9$ triquadratic finite elements ($3 \cdot 90$ of them are outside the trimmed domain). Only a section of the grid in the xz-plane is shown. Using a pcg solver, the system was solved to a relative accuracy of $< 1E - 10$ in less than 600 iterations.

The efficiency of b-spline algorithms, demonstrated by the above examples, is also reflected in the simplicity of finite element codes. The beauty of b-spline programming is particularly evident for multigrid techniques [11], where subdivision serves as canonical grid transfer.

9 Conclusion

Comparing Figures 5, 6, and 7, the various basis functions are qualitatively very similar. Perhaps this is not too surprising; after all, each of the slightly different concepts is based on b-splines. As a consequence, the finite elements share many advantages:

- free choice of smoothness and order of accuracy
- efficient recurrences for basic operations
- flexible geometry representation
- vectorized algorithms and multilevel techniques
- simple data structure with one node per grid point
- natural adaptive refinement via hierarchical bases

With many common favorable features, weighted and isogeometric methods both perform well for a broad range of applications. However, there are some pros and cons which we would like to point out below.

If a natural weight function is available, like for constructive solid geometry models or for many problems in linear elasticity, weighted approximations suggest themselves. Another ideal application are free boundary problems, where the unknown boundary can be implicitly represented by a spline serving as a weight function which changes with time.

On the negative side, the numerical construction of weight functions from boundary representations can be difficult, particularly in three dimensions. General purpose schemes have to rely on efficient algorithms for computing the distance function in a neighborhood of the domain boundary.

Isogeometric techniques are the method of choice if a CAD description of the domain D as solid model without trimming is available. This means that D is already partitioned into moderately deformed rectangles and cubes, respectively. If this is not the case, depending on the topological structure of D, the domain decomposition can be nontrivial. There is some similarity to the generation of coarse hexahedral meshes. Of course, we could also allow triangles and tetrahedra as additional parameter domains. But then, the isogeometric method loses some of its computational efficiency.

Numerical integration is crucial for both techniques. Isogeometric methods require only integration over grid cells, an ideal situation. However, the evaluation of integrands of the form (3) is time consuming. Hence, minimal node formulas are especially important. Weighted methods have simpler integrands. Yet, the integration over boundary cells is nontrivial. To preserve the high accuracy of the b-spline approximations, cells which are intersected by the domain boundary must be partitioned into smooth images of standard domains. Fortunately, topologically difficult intersection patterns are less frequent so that they do not have a significant impact on the overall computing time.

The mixed method introduced in this paper eliminates some of the difficulties mentioned above. Figure 7 serves as a typical example. Boundary integration is necessary only for grid cells with relatively simple intersection patterns. Moreover, despite the nontrivial shape of the domain, computations use a parametrization over a single rectangle.

As is apparent from the above remarks, there are numerous topics for future research. With a joint effort, continued progress will be made, and we believe that b-splines have the potential to become a standard in finite element analysis, too.

Acknowledgements. We thank Ulrich Reif and Joachim Wipper, the co-founders of the web-method, for a continuing excellent cooperation. Moreover, we gratefully acknowledge the support by the numerical analysis group in Stuttgart. In particular, we thank Christian Apprich for valuable suggestions and for maintaining our two-dimensional web-software. As usual, Mrs. Walter helped us with a careful reading of our manuscript.

References

1. Apaydin, G.: Finite Element Method with Web-splines for Electromagnetics. VDM Verlag, Saarbrücken (2009)
2. Bazilevs, Y., Beirão da Veiga, L., Cottrell, J.A., Hughes, T.J.R., Sangalli, G.: Isogeometric Analysis: Approximation, stability and error estimates for h-refined meshes. Math. Models Meth. Appl. Sci. 16, 1031–1090 (2006)
3. Bazilevs, Y., Calo, V.M., Cottrell, J.A., Evans, J., Lipton, S., Hughes, T.J.R., Scott, M.A., Sederberg, T.W.: Isogeometric Analysis using T-Splines. Comput. Methods Appl. Mech. Engrg. 199, 229–263 (2010)
4. Bazilevs, Y., Calo, V.M., Hughes, T.J.R., Zhang, Y.: Isogeometric fluid-structure interaction: Theory, algorithms and computations. Comput. Mech. 43, 3–37 (2008)
5. de Boor, C.: A Practical Guide to Splines. Springer, New York (1978)
6. Calderón, A.P.: Lebesgue spaces of differentiable functions and distributions. Proc. Symp. in Pure Math. 4, 33–49 (1961)
7. Cottrell, J.A., Hughes, T.J.R., Bazilevs, Y.: Isogeometric Analysis: Toward Integration of CAD and FEA. Wiley, Chichester (2009)
8. Gomez, H., Hughes, T.J.R., Nogueira, X., Calo, V.M.: Isogeometric analysis of the isothermal Navier-Stokes-Korteweg equations. Comput. Methods Appl. Mech. Engrg. 199, 1828–1840 (2010)
9. Hoffacker, A.: Gewichtete Isogeometrische Finite Elemente mit B-Spline-Ansatzfunktionen. Master Thesis, Stuttgart (2011)
10. Höllig, K.: Finite Element Methods with B-Splines. SIAM, Philadelphia (2003)
11. Höllig, K., Hörner, J.: Programming multigrid algorithms with b-splines (in preparation)
12. Höllig, K., Reif, U., Wipper, J.: Weighted extended B-spline approximation of Dirichlet problems. SIAM J. Numer. Anal. 39, 442–462 (2001)
13. Höllig, K., Hörner, J., Pfeil, M.: Parallel finite element methods with weighted linear b-splines. In: Nagel, W.E., Kröner, D., Resch, M. (eds.) High Performance Computing in Science and Engineering 2007, pp. 667–676. Springer, Heidelberg (2008)
14. Hughes, T.J.R., Cottrell, J.A., Bazilevs, Y.: Isogeometric analysis: CAD, finite elements, NURBS, exact geometry, and mesh refinement. Comput. Methods Appl. Mech. Engrg. 194, 4135–4195 (2005)
15. Kantorowitsch, L.W., Krylow, W.I.: Näherungsmethoden der Höheren Analysis. VEB Deutscher Verlag der Wissenschaften, Berlin (1956)
16. Mößner, B., Reif, U.: Stability of tensor product b-splines on domains. J. Approx. Theory 154, 1–19 (2008)
17. Rvachev, V.L., Sheiko, T.I.: R-functions in boundary value problems in mechanics. Appl. Mech. Rev. 48, 151–188 (1995)
18. Schumaker, L.L.: Spline Functions: Basic Theory. Wiley-Interscience, New York (1980)
19. Stein, E.M.: Singular Integrals and Differentiability Properties of Functions. Princeton University Press, Princeton (1970)
20. Strang, G., Fix, G.J.: An Analysis of the Finite Element Method. Prentice–Hall, Englewood Cliffs (1973)
21. Zienkiewicz, O.C., Taylor, R.I.: Finite Element Method, vol. I–III. Butterworth & Heinemann, London (2000)